SCANNING VOL. 24, 000–000 (2002)

Received: February 27, 2002
Accepted with revision: August 28, 2002

The Two-Dimensional and Three-Dimensional Processing of Images Provided by Conventional Microscopes

DALIBOR MARTIŠEK

Department of Mathematics, Faculty of Mechanical Engineering, Brno University of Technology, Brno, Czech Republic

Summary: In this paper, I present an interesting processing method of microscopic images. High-pass type filters are generally used for image focusing. They enhance the high spatial frequencies. They are, however, efficient only in cases when the picture is not sharp because of the low contrast on high frequencies (for example in a TV picture). These filters, are not appropriate if the lack of sharpness has been caused by other factors. In this case, it is not possible to construct a three-dimensional model of the observed object. Better results and a three-dimensional model can be obtained by applying the following theory. As part of this paper, an original program based on this theory is described.

Key words: graphic plane, physical pixel, multifocal image, Euclidean trace of point, focusing criterion

PACS: 07.60.Pb, 07.79.-v

1.0 Introduction

In computer graphics, data are stored as the coordinates of points. Points are viewed as nondimensional objects conforming to the traditional Euclidean geometry. The display surface of an output device is, however, a physical object and cannot display dimensionless points. For this reason, the notion of "pixel" rather than point is used, denoting the smallest viewable formation. In mathematical modelling, however, pixels in the logical sense have to be considered (i.e. the output device is thought of as a set of isolated Euclidean points) in contrast to the physical sense (where the output device is taken to represent a set of elementary small surfaces). In the present literature, these differences are often ignored. Nevertheless, even in cases where these notions are differentiated, their definitions are very vague and sometimes even false. To allow for all possible constructions, it is very important to give an exact definition of pixel.

In the following, we will provide a mathematical model of the entire situation.

2. Graphic Plane

2.1. Definition

Let $I = \langle i_1;i_2)$; $J = \langle j_1;j_2)$ be intervals. Further let $D_x = \{x_i\}_{i=0}^{m}$; $m > 1$ be an equidistant division of I, $D_y = \{y_i\}_{i=0}^{n}$; $n>1$ an equidistant division of J. The rectangle $\mathbf{F}_{ij} = \langle x_i;x_{i+1}) \times \langle y_j;y_{j+1})$; $i = 0,1,..,m-1$, $j = 0,1..,n-1$, will be called a physical pixel. The number $p_x = x_{i+1}-x_i$ or $p_y = y_{j+1}-y_j$ will be called the horizontal or the vertical dimension of the physical pixel $\mathbf{F}_{ij}$, respectively. The rectangle $I\times J$ together with divisions D_x, D_y is called a graphic plane, denoted by $\mathcal{G}_2$, or in detailed notation, $\mathcal{G}_2 = (I\times J,D_x,D_y)$. We will call the ordered pair $(m;n)$ the graphic plane resolution.

The theorem shown below follows directly from this definition:

2.2. Theorem

The set $\mathcal{F}_2 = \{\mathbf{F}_{ij} = \langle x_i;x_{i+1}) \times \langle y_j;y_{j+1}) \mid i \in \{0,..,m-1\}; j \in \{0,..,n-1\}\}$ of all physical pixels in the graphic plane $\mathcal{G}_2$ is a representation of $\mathcal{G}_2$.

By the definition, all the vertical and horizontal vertical sizes of the physical pixels $\mathbf{F}_{ij}$ in $\mathcal{G}_2$ are equal. This immediately proves the following theorem:

2.3. Theorem

Let $\mathcal{G}_2$ be an arbitrary graphic plane, $\mathcal{F}_2$ the set defined in 2.2. The relation ρ defined on $\mathcal{G}_2$ by $\rho(A,B) \Leftrightarrow (\exists \mathbf{F}_{ij} \in \mathcal{F}_2)[A \in \mathbf{F}_{ij} \wedge B \in \mathbf{F}_{ij}]$ is an equivalence on $\mathcal{G}_2$.

This project is supported by research design CEZ: J22/98:261100009 "Non-traditional methods for investigating complex and vague systems".

Address for reprints:

Dalibor Martišek
Department of Mathematics
Faculty of Mechanical Engineering
Brno University of Technology
Technicka 2
CZ-61669 Brno, Czech Republic
e-mail: martisek@mat.fme.vutbr.cz

2.4. Definition

Let $\mathcal{G}_2$ be a graphic plane. The factor set $\mathcal{F}_2 = \mathcal{G}_2/\rho$, where ρ is the equivalence from the previous theorem, is called the physical plane of $\mathcal{G}_2$. Under the resolution of the physical plane $\mathcal{F}_2$ we understand the resolution of the corresponding graphic plane $\mathcal{G}_2$.

To model a graphic plane we can use virtually any output device such as a monitor, printer, and so forth.

2.5. Definition

Let $\mathcal{F}_2$ be a physical plane, $\mathbf{F}_{ij}$ its physical pixels. The ordered pair $[i,j]$ is called the coordinates of $\mathbf{F}_{ij}$.

2.6. Definition

Let $\mathcal{F}_2$ be a physical plane and $C_r = \{c \in N;\ 0 \le c \le r;\ r > 1\}$. A mapping $O: \mathcal{F}_2 \to C_r$ is called an image matrix or short an image. The set C_r is called an r-chromatic set. If $O: \mathbf{F}_{ij} \to c$, c is called the value or colour of $\mathbf{F}_{ij}$. Under the resolution of the image we understand the resolution of the incident physical plane.

Next, it is obvious that the following theorem holds:

2.7. Theorem

Let $\mathcal{G}_2$ be a graphic plane, $\mathcal{F}_2$ its physical plane, $\mathbf{F}_{ij}$ its physical pixels. The mappings

$$^{(2)}\mathscr{E}_{\mathcal{F}} : \mathcal{F}_2 \times \mathcal{F}_2 \to \mathbf{R} \text{ such, that}$$
$$^{(2)}\mathscr{E}_{\mathcal{F}}(\mathbf{F}_{ij};\mathbf{F}_{kl}) = \sqrt{(k-i)^2 + (l-j)^2};$$

$$^{(2)}\mathscr{P}_{\mathcal{F}} : \mathcal{F}_2 \times \mathcal{F}_2 \to \mathbf{R} \text{ such, that}$$
$$^{(2)}\mathscr{P}_{\mathcal{F}}(\mathbf{F}_{ij};\mathbf{F}_{kl}) = |k-i| + |l-j|;$$

$$^{(2)}\mathscr{C}_{\mathcal{F}} : \mathcal{F}_2 \times \mathcal{F}_2 \to \mathbf{R} \text{ such, that}$$
$$^{(2)}\mathscr{C}_{\mathcal{F}}(\mathbf{F}_{ij};\mathbf{F}_{kl}) = \max\{|k-i|;|l-j|\};$$

are metrics on $\mathcal{F}_2$.

2.8. Definition

Let $\mathcal{G}_2$ be a graphic plane, $\mathcal{F}_2$ its physical plane, $\mathbf{F}_{ij}$ its physical pixel. The Mappings $^{(2)}\mathscr{E}_{\mathcal{F}}$; $^{(2)}\mathscr{P}_{\mathcal{F}}$; $^{(2)}\mathscr{C}_{\mathcal{F}}$ from Theorem 2.7. are called a Euclidean, postman, and square metric on $\mathcal{F}_2$, respectively.

For its computational simplicity, the square metric is used in image processing. For sophisticated graphic algorithms and other applications, mostly other metrics are used (e.g. for three-dimensional [3-D] reconstruction).

3. Mathematical Model of a Conventional Microscope

In geometrical optics, terms such as object space and image space are used. In the sequel, we will use a mapping that conforms to the postulates of geometrical optics and call it a geometrical projection. The mapping is implemented by direct rays that pass through the point P that is to be displayed. These rays are transformed by the optical system into conjugated rays that pass through the image space and meet at a point P'.

However, the mapping as implemented by a real conventional microscope does not conform exactly to the postulates of geometrical optics. The following is a list of some of the reasons for this:

The limited width of the beam of rays: The mapping of point P is carried out by a beam of rays. If we denote by $\mathcal{A}$ the set of the values assumed by the angles formed by the rays of the bunch, then $\sup \mathcal{A} = \pi$. Although the beam of rays that enter into the lens is very broad, since it must always carry enough light with a real microscope we have always $\sup \mathcal{A} < \pi$. Thus by S we shall denote the beam of rays that really goes through the optical microscope.

The wave nature of light: Geometric optics presumes, that light propagates along straight lines. This presumption, however, is valid only if light goes through a homogeneous and isotropic environment (which, in a microscope, can be presumed), and further if light passes obstacles that are larger than its wavelength by orders of magnitude. This, however, is not the case with microscopes. When a microscopic a microscopic preparation is observed, light is always inflected by a small obstacle—the preparation itself. The optical system of the microscope as such also produces flexural phenomena, namely, on the input pupil. Thus, to give a mathematical description of an optical microscope we must also take into account the wave nature of these phenomena. This means that the geometrical projection $\mathcal{G}: P_3 \to P_3'$ cannot be used and has to be replaced by a more general correspondence between the object and image space; strictly speaking between the sharpness plane ω and the ocular focal plane φ_2:

3.3. Definition

Let $\mathcal{M}_v \subset \omega \times \varphi_2$ be a relation such that $[P;Q] \in \mathcal{M}_v \Leftrightarrow Q \in \mathscr{S}_V^P = \left\{ X \in \varphi_2 \,\middle|\, |XP'| \le \frac{\lambda_0}{4A} \wedge P' = \mathcal{G}(P) \right\}$ $\mathcal{M}_v$ is called wave scanning. The set $\mathscr{S}_V^P$ is called the wave trace of the point P, the number $d(\mathscr{S}_V^P) = \sup_{X,Y \in \mathscr{S}_V^P} \{a \in R | a = |X;Y|\} = \frac{\lambda_0}{2A}$ is called its average. (A is the so-called numerical aperture of the microscope, λ_0 the wave length of light used.) The wave trace of the point is illustrated in Fig. 1.

Nonplanarity of the preparation: As indicated above, it follows that it is impossible to focus the microscope so that it displays the point as a point. When observing a nonpla-

nar preparation, further problems are encountered. As mentioned before, for an image of the preparation to be sharp, the preparation must be placed exactly in the plane to which the microscope is focussed. This plane is called a sharpness plane. However, in many cases, we cannot take the preparation to be a plane, and therefore these conditions cannot be fulfilled. The sharpness plane intersects the 3-D preparation in a contour line. The points of this contour line will be displayed with maximum possible sharpness. The points of the preparation that lie outside this plane cannot be displayed as points, even if we abstract from the wave nature of light and assume its straight propagation (see Fig. 2).

3.4. Definition

Let P_3 be the object space of a microscope, $\mathcal{G}$: $P_3 \to P_3'$ a geometrical projection. Further let $\bar{P} \in P_3$; $\mathcal{G}$: $\bar{P} \to \bar{P}'$; S be the homocentric bunch gone thorough the point $\bar{P}$ and $\mathcal{G}$: $S \to S'$. The relation $\mathcal{M}_E \subset P_3 \times \varphi_2 = \left\{ \left[\bar{P}; \bar{P}' \right] \middle| \exists \bar{p} \in S' : \bar{P}' \in \bar{p} \cap \varphi_2 \right\}$ is called Euclidean scanning. We will call the set $\mathcal{S}_E^P = \left\{ P' \in \varphi_2 \middle| [P; P'] \in \mathcal{M}_E \right\}$ the Euclidean trace of the point P, and the number $d\left(\mathcal{S}_E^P\right) = \sup\left\{ |X;Y|; X, Y \in \mathcal{S}_E^P \right\}$ its average.

If we view the image of point P from the object focal plane of the ocular, then the Euclidean scanning translates this point into its trace whose average is generally greater than zero, even if straight propagation of light is assumed (see Fig. 3).

Scanner resolution: In all the above considerations of the properties of an optical microscope, we assumed that all the

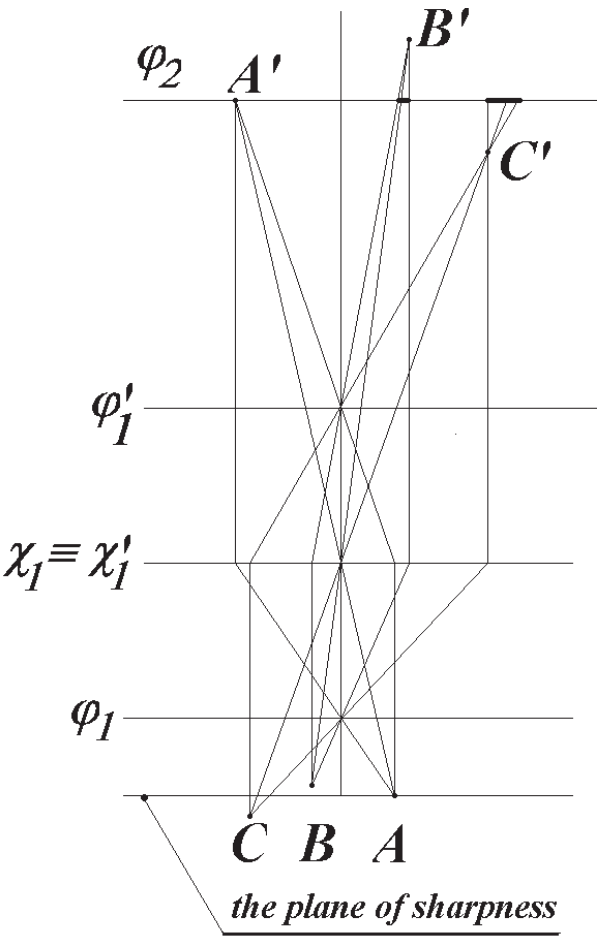

FIG. 2 Nonplanarity of the preparation.

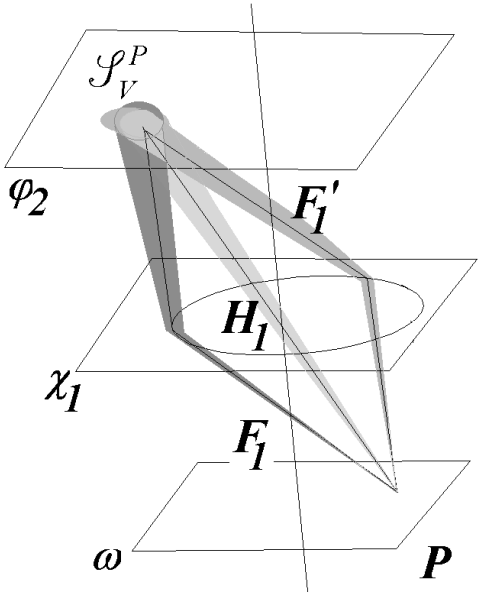

FIG. 1 Wave trace of the point.

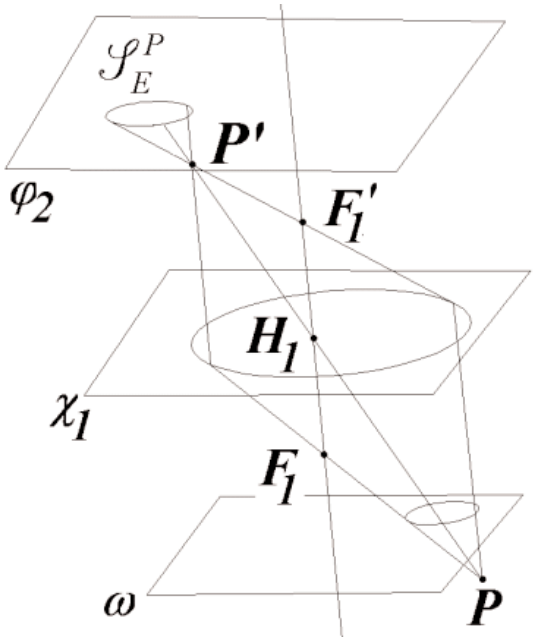

FIG. 3 Euclidean trace of the point.

deviations from the geometrical projection originate in the microscope during the projection itself. However, these deviations are also caused by the scanner. Assuming the straight propagation of light let the preparation being placed flush with the microscope sharpness plane, then the geometrical projection $\mathcal{G}$ takes every point $P \in \omega$ of the preparation to point $P' \in \varphi$. Despite this, this point cannot be mapped to a point. A scanner is a physical object and, therefore, it cannot represent the point as a dimensionless object. No matter on which principle the scanner works, it more or less meets the criteria of a graphic plane, as described in the definitions starting by 2.1. Every point is displayed as a physical pixel with nonzero dimensions, and its particular value depends on the size and resolution $(w;h)$ of the scanner.

The image acquired by a particular scanner from a particular microscope is the result of intricate interactions of the phenomena described above. An accurate mathematical description of these interactions would be extremely complicated. However, as will be demonstrated in the following, there are interesting possibilities of reconstructing real images.

4. Zone of Sharpness, Multifocal Image

In the previous chapter, we indicated that in a nonplanar preparation only the contour line, in which the preparation intersects the sharpness plane, is displayed sharply. However, in such a case, any nonplanar preparation would be virtually out of focus. On the other hand, in real images resulting from conventional microscopes, the parts that are in focus are perfectly sharp with only the rest out of focus (see Fig. 4), with microphotographs of an *Astrophy-*

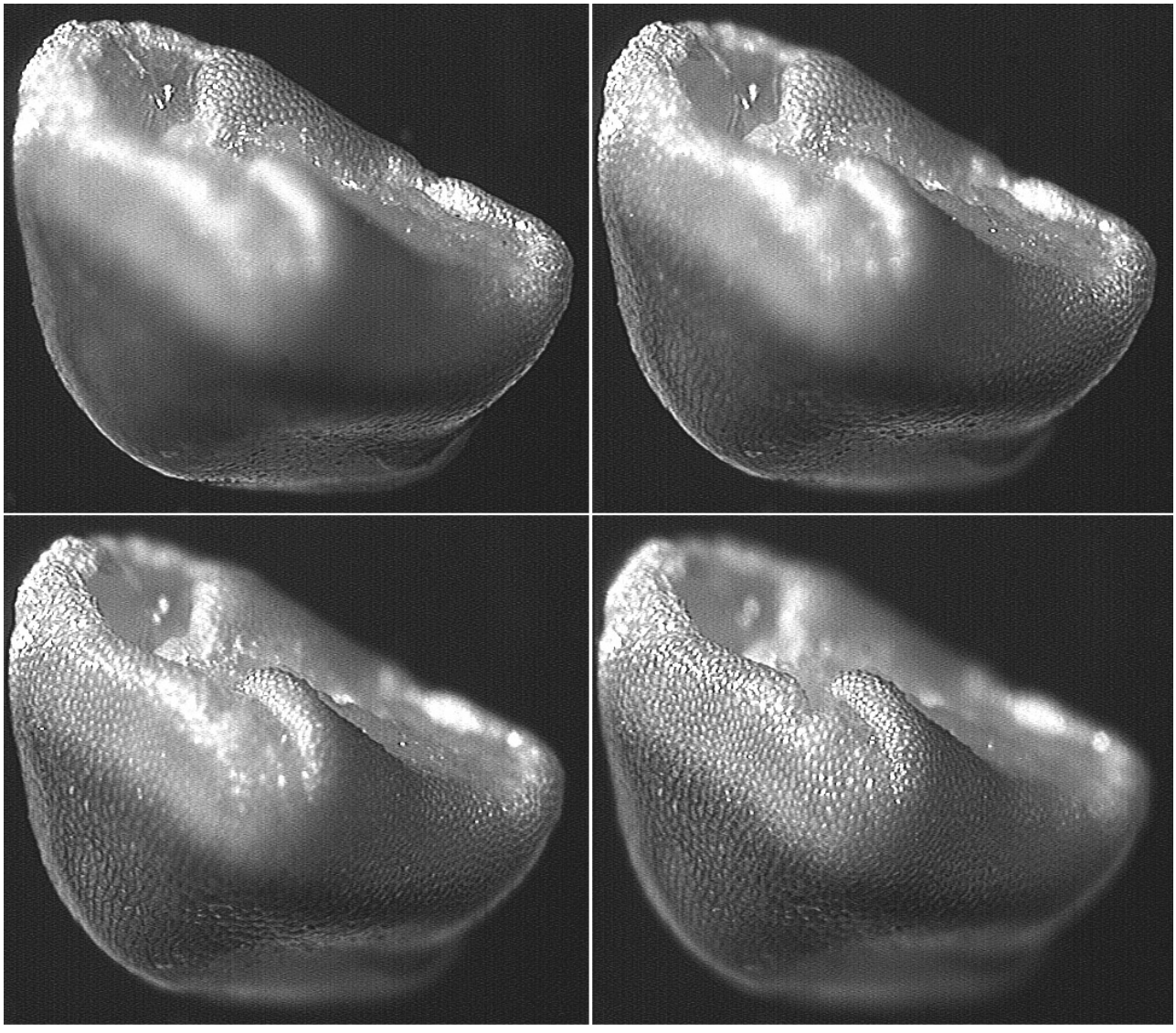

FIG. 4 Different optical cuts of the preparation.

tum Ornatum cactus seed taken at different focal planes where the focussed parts of the image are well discernible. The conclusions concerning the focalisation contour line are based on the assumption that the sharpness level and the focal plane are Euclidean planes, but this assumption is not valid.

If the point to be displayed lies outside the sharpness plane, it is displayed into its Euclidean trace, whose radius depends on the distance of the point from the plane. As the distance is increased, so is the radius. However, the dependence is not proportional. If it were possible to display Euclidean points in the plane, then every nonzero Euclidean trace would cause a defocussed image.

If the plane of a scanning device is a set of physical pixels, then the unsharpness is only demonstrated if $d(\mathscr{S}_E^P)>p$ where $p = \min\{p_x;p_y\}$. If $d(\mathscr{S}_E^P)\le p$, we can take the picture for sharp.

4.1. Definition:

Let $P \in P_3$ be a point of an objective space, $\mathscr{M}_E \subset P_3 \times \varphi$ an Euclidean scanning, $\mathcal{F}_2$ the physical plane of the focal plane φ, $p_x;p_y$ the dimension of its physical pixels, $d(\mathscr{S}_E^P)$ the diameter of the Euclidean trace of point P. We call the set ${}_{(O)}P_3 = \{P \in P_3 \mid d(\mathscr{S}_E^P) < p; p = \min\{p_x;p_y\}\}$ an open zone of sharpness. Its image ${}_{(O)}P_3'$ in the geometrical projection $\mathcal{G}:{}_{(o)}P_3 \to {}_{(O)}P_3'$ is called an optical cut.

It is evident that the result of a scanning depends not only on the preparation that is observed, but also on the microscope focalisation. The same preparation may be observed with different focalisations, that is, with different settings of the focal planes. If the number of these settings is generally n, we will get n different scannings and n different optical cuts ${}_{(O)}P_3'$ of the preparation. It is evident that it is only possible to obtain a sharp image by a single scanning, if the zone of sharpness is wider then the preparation height. If, however, it is smaller than the preparation height, part of the preparation is always out of focus (in Fig. 4. we can see different optical cuts of the *Astrophytum Ornatum* cactus seed). To construct a sharp picture in such a case, a multifocal image is required. This is a sequence of images whose zones of sharpness cover the whole preparation height.

4.2. Definition

Let $\{{}^{(k)}\mathscr{M}_E\}; k = 1,..,n$ be a sequence of Euclidean scanning of the same preparation $\mathscr{P}$, $\{{}^{(k)}_{(O)}\overline{P}^3\}; k = 1;..;n$ a sequence of its sharpness zones where $\mathscr{P} \subset \bigcup_{k=1}^{n} {}^{(k)}_{(O)}\overline{P}^3$. The sequence $\{{}^{(k)}O\}; k = 1,..,n$ of the scanning results is called a multifocal image (or, more precisely, an n-focal image).

The two-dimensional (2-D) processing of an n-focal image obviously involves constituting new image so that this new image consists of the optical cuts of the images $\{{}^{(k)}O\}; k = 1,..,n$.

5. Focussing Criteria

In the next step, we will fix criteria for assigning each pixel in the images $\{{}^{(k)}O\}; k = 1,..,n$ to an optical cut ${}_{(O)}P_3'$. Human eyes can see a part of the image sharply when the brightness of near points differs significantly. To identify the most focussed part and to construct a sharp image, it is necessary to analyse the magnitude dependent on these differences – the so-called focussing criteria. First, the focussing of a physical pixel has to be formally defined:

5.1. Theorem

Let $K_{ij} = (\mathbf{F}_{ij};r)$ be a circle in an arbitrary metric of the scanner physical plane $\mathcal{F}_2$, ${}^{(k)}P_{ij}:K_{ij} \to C_n$ a subimage of the image ${}^{(k)}O$ from the n-focal image $\{{}^{(k)}O\}$; $k = 1,..,n$, and $\mathscr{S}_{ij} = 2^{K_{ij}}$ be a set of all the subset of circle K_{ij}. Furthermore, let ${}^{(k)}C_{rs}$ be the value of the physical pixel $\mathbf{F}_{ij}$ in the image ${}^{(k)}O$ and let ${}^{(k)}C = \sum_{K_{rs}} {}^{(k)}C_{rs}$ be a sum over the values of K_{ij} in the image ${}^{(k)}O$. Let ${}^{(k)}P:\mathscr{S}_{ij}$ be a mapping, where

a) $${}^{(k)}P\left(\{\mathbf{F}_{rs}\}\right) = \frac{{}^{(k)}C_{rs}}{{}^{(k)}C}$$

b) $$A, B \in \mathscr{S}_{ij} \wedge A \cap B = \varnothing \Rightarrow {}^{(k)}P\left(\{A \cup B\}\right) = {}^{(k)}P\left(\{A\}\right) + {}^{(k)}P\left(\{B\}\right)$$

Then $(K_{ij};\mathscr{S}_{ij};{}^{(k)}P); k = 1,..,n$ are probability spaces and the mappings ${}^{(k)}X:K_{ij}\to\mathbf{R}$: ${}^{(k)}X\left(\{F_{rs}\}\right) = \frac{{}^{(k)}C_{rs}}{{}^{(k)}C}$ are discrete integrable random variables.

5.2. Definition

The mappings ${}^{(k)}X:K_{ij} \to \mathbf{R}$; $k=1,2,..,n$ in the previous theorem are called the focussings of the physical pixel $\mathbf{F}_{ij}$ in the image ${}^{(k)}O$.

Variation span, variance, high spatial frequency amount in the sense of the Fourier transformation can all be used as focussing criteria.

The mean values of the defined focussings are $E({}^{(k)}X) = \sum_{K_{ij}} \frac{{}^{(k)}C_{rs}}{{}^{(k)}C}$ and the value range is

$$v\left({}^{(k)}X\right) = \frac{1}{{}^{(k)}C}\left(\max_{\mathbf{F}_{rs}\in K_{ij}}\left\{{}^{(k)}C_{rs}\right\} - \min_{\mathbf{F}_{rs}\in K_{ij}}\left\{{}^{(k)}C_{rs}\right\}\right) \quad (1)$$

The mappings ${}^{(k)}Y = ({}^{(k)}X - E({}^{(k)}X))^2 : K_{ij}\to\mathbf{R}$, where

$${}^{(k)}Y\left(\mathbf{F}_{rs}\right) = \left(\frac{{}^{(k)}C_{rs}}{{}^{(k)}C} - \sum_{K_{ij}} \frac{{}^{(k)}C_{rs}}{{}^{(k)}C}\right)^2; k = 1,2,..,n,$$

are also discrete integrable random variables, and

$$D\left({}^{(k)}X\right)=\frac{1}{{}^{(k)}C}\sum_{K_y}\left(\frac{{}^{(k)}C_{rs}}{{}^{(k)}C}-\sum_{K_{ij}}\frac{{}^{(k)}C_{rs}}{{}^{(k)}C}\right)^2 \qquad (2)$$

are dispersions of random variables ${}^{(k)}X$ defined on circle K_{ij} in the scanner physical plane $\mathcal{F}_2$.

To construct the last criterion, we use a Fourier transform. If $\mathcal{D}: \{{}^{(k)}C_{rs}\} \rightarrow \{{}^{(k)}X_{mn}\}$ is a discrete Fourier transform where ${}^{(k)}C_{rs}$ is the value of the processed pixel $\mathbf{F}_{ij}$ in image k, ${}^{(k)}X_{mn} = {}^{(k)}U_{mn} + i^{(k)}V_{mn}$; $m,n = 0,1,..,2\varepsilon$, then the expressions $\left|{}^{(k)}X_{mn}\right| = \sqrt{{}^{(k)}U_{mn}^2 + {}^{(k)}V_{mn}^2}$ determine the amplitudes of the spatial frequencies that exist in the neighbourhood K_{ij} of the physical pixels $\mathbf{F}_{ij}$ in the particular images ${}^{(k)}O$, $k = 1,2,..,n$. Higher values of indices m,n mean higher spatial frequencies, which indicate a higher contrast of small details in the surveyed surrounding and thus also a better focussing. Therefore, as a focussing criterion, the expression containing the frequency $|{}^{(k)}X_{mn}|$ may be used, that assigns higher weight to higher indicies m,n. To identify the sharpness zone, we particularly used the expression

$${}^{(k)}T(X_{mn})=\sum_{m=0}^{H}\sum_{n=0}^{H}(m+n)\sqrt{{}^{(k)}U_{mn}^2+{}^{(k)}V_{mn}^2}; H \le \varepsilon \qquad (3)$$

I call this expression a frequency criterion.

The maxima of the Eqs. (1), (2), and (3), called a variation, dispersal, and frequency criterion, respectively, detect the pixels focussed at a maximum very well and thus may be used to compose a sharp picture.

Fig. 5a shows the sharpness zones detected by Eq. (1) for a multifocal image composed of four images (the first and the fourth can be seen in Fig. 4). A sharp image is constructed in 5b.

6. Logical Pixels, Mapping

A physical pixel can be thought of as the smallest object distinguished by the given equipment. The set of all the physical pixels is called a physical plane.

6.1. Definition

Let $\mathcal{G}_2$ be a graphic plane. The factor set $\mathcal{F}_2 = \mathcal{G}_2/\rho$ where the relation ρ is defined as $\rho(A,B) \Leftrightarrow (\exists F_{ij} \in \mathcal{F}_2)$ $\lfloor A \in F_{ij}\, B \in F_{ij} \rfloor$ is called the physical plane of $\mathcal{G}_2$.

In many graphical applications, a so-called logical plane and logical pixels have to be used. Sometimes it is important to which (Euclidean) point of the physical pixel we refer — its centre, vertex, and so forth. Thus, by a logical pixel L_{ij} we mean a representative of the physical pixel $\mathbf{F}_{ij}$, the logical plane $\mathcal{L}$ being the set of all the logical pixels $\mathcal{L}$:

6.2. Definition

Let $\mathcal{G}_2$ be a graphical plane, $\mathcal{F}_2$ its physical plane, p_x or p_y the dimensions of its physical pixels F_{ij} respectively. Let

$$\text{for } c \in \langle 0;1)\ {}_cW = \left\{r_i \in \mathbf{R} \middle| \forall i \in \{0,1,...,w-1\} : r_i \in \langle i; i+1) \wedge r_i - k = c\right\} \text{ and}$$

$$\text{for } d \in \langle 0;1)\ {}_dH = \left\{s_j \in \mathbf{R} \middle| \forall j \in \{0,1,...,h-1\} : s_j \in \langle j; j+1) \wedge s_j - k = d\right\},$$

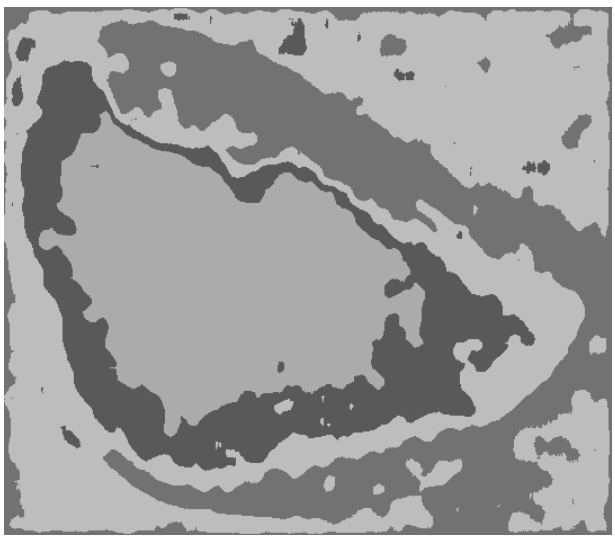

(a)

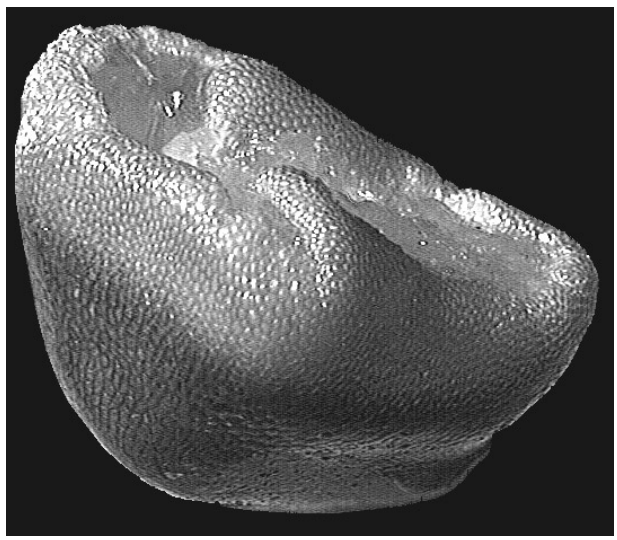

(b)

FIG. 5 Optical cuts detected by the Eq. (1) and focussed image constructed from the optical cuts.

and $P = [c,d]$. Then the set ${}_p\mathcal{L} = {}_cW \times {}_dH$ is called a logical plane, the ordered pair $(w;h)$ its resolution, and its elements logical pixels.

The below theorem follows directly from definitions 6.1. and 6.2.:

6.3. Theorem

Let $\mathcal{F}_2$ be the physical plane of the graphical plane $\mathcal{G}_2$, ${}_p\mathcal{L}_2$ any logical plane of the same graphical plane, ${}_p\varphi: \mathcal{F}_2 \to {}_p\mathcal{L}_2$ a mapping where, for all $i = 0,1,..,m-1$, $j = 0,1,..,n-1$, ${}_p\varphi(F_{i,j}) = {}_pL_{i,j} \Leftrightarrow {}_pL_{i,j} \in F_{i,j}$. Then the mapping ${}_p\varphi$ is a bijection (one-to-one and onto mapping).

6.4. Definition

The mapping ${}_p\varphi: \mathcal{F}_2 \to {}_p\mathcal{L}_2$ in the previous theorem is called a mapping of the physical plane. The mapping from Def. 6.4 is illustrated in Fig. 6.

It is evident that, for each physical plane, an infinite number of logical planes exist since a logical plane ${}_p\mathcal{L}_2$ may be constructed for any $P = [c,d] \in \langle x_0;x_1) \times \langle y_0;y_1)$. Every physical plane can be mapped in an infinite number of ways. In the sequel, I will only use the two most important mappings.

6.5. Definition

The mapping ${}_v\varphi: \mathcal{F}_2 \to {}_v\mathcal{L}_2$, where $V = [x_0;y_0]$, is called a vertex mapping. The mapping ${}_s\varphi: \mathcal{F}_2 \to {}_s\mathcal{L}_2$, where

$$S = \left[\tfrac{1}{2}(x_0 + x_1); \tfrac{1}{2}(y_0 + y_1)\right],$$

is called a centre mapping.

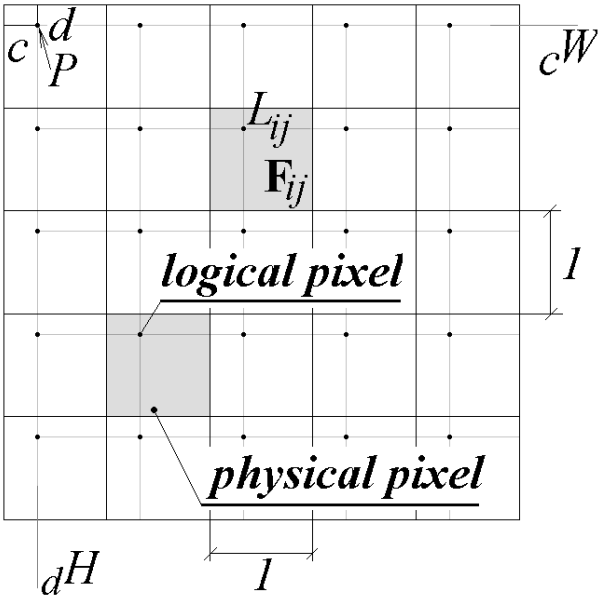

FIG. 6 Mapping of the physical plane.

In this paper we will only concern ourselves with the construction of objects whose surface can be thought of as the graph of a function of two variables $z = f(x;y)$ defined on a rectangle $\langle x_1;x_2\rangle \times \langle y_1;y_2\rangle$. Any computer output device is a physical plane with a finite number of physical pixels. Therefore, it is not possible to construct on it a function continuous in terms of the ordinary definition. Regarding its construction on a computer, any definition of the above-mentioned continuous function is equivalent to assigning values to the logical or physical pixels of the function's domain. This raises the question of how such a function can be constructed.

Two possibilities exist:

1. *The definition set can be thought of as a not mapped physical plane.* If the definition set is a rectangle $\langle x_1;x_2\rangle \times \langle y_1;y_2\rangle \in \mathbf{R}^2$, it is possible to construct equidistant divisions $D_x = \{x_i\}_{i=0}^m$; $m>1$, $D_y = \{y_i\}_{i=0}^n$; $n>1$ of intervals $\langle x_1;x_2\rangle$, $\langle y_1;y_2\rangle$ and thereby a graphic plane and its physical plane as well. To the whole of a physical pixel we assign a constant value, and a 3-D object is composed of blocks (or of theirs surfaces) whose bases are the physical pixels and heights are their values.

It is relatively easy to construct such a surface, but it involves many disadvantages. If the value of a pixel, however, is taken for its height, then the graph of the function $z = f(x,y)$ is modelled as a 3-D surface. This "physical function," however, is not suitable for 3-D reconstructions because with only three normals existing, the figure after shading gives a very unnatural impression (see Fig. 7).

2. The definition set is equipped with a suitable mapping: In this case, the surface is constructed by interpolating the graph of a function in two variables where the function values are known at equidistant points (see Fig. 8). The shading value of a 2-D plane segment is given by the cosine of the angle at which the segment's normal intersects the incident light, which is constant for a 2-D segment. However, if we really paint the whole constructed plane segment with the same colour (the so-called constant shading), the segment edges become visible to the naked eye over all the

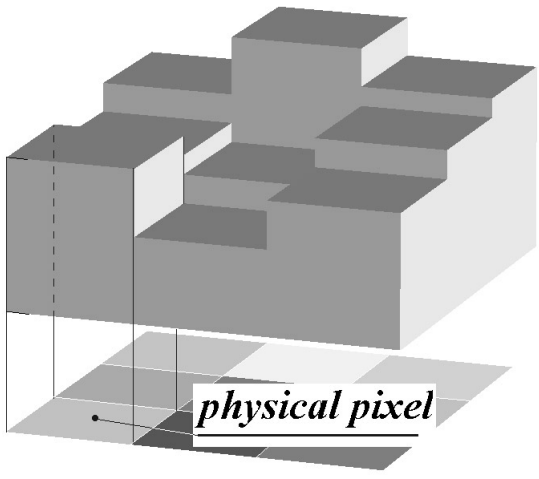

FIG. 7 The definition set of a function as not mapping physical plane.

originally smooth surface, which, improperly, stresses the fact that the constructed segment assumed to be smooth is, in fact, an interpolation (sometimes a very coarse one). This unpleasant effect can be improved by interpolating either the colour or the normal.

8. Spatial Reconstruction by the Method of Constant High Cuts and Filtered Cuts

Let ${}^{(k)}O$; $k = 1,..,n$ be a particular image of the multifocal image O, $\mathbf{F}_{ij}$ its physical pixel, ${}^{(0)}O$ the image, which is ${}^{(0)}O(\mathbf{F}_{ij}) = k$. From the way a multifocal picture is generated, it is evident that, if ${}^{(0)}O(\mathbf{F}_{ij}) = k$, then the physical pixel $\mathbf{F}_{ij}$ contains information about the point P of the preparation for which $P \in {}^{(k)}P$; $k = 1,..,n$. If the zones ${}^{(k)}P$; $k = 1,..,n$ are mutually disjointed, each point in the zone ${}^{(k)}P$ can be assigned an identical height. Thus, we obtain a function of two variables whose graph approximately matches the observed preparation. If we denote by v the total height of the preparation, then the zone sharpness height of a n-focal picture is $\frac{v}{n}$. For the function $f(i,j)$, which approximately describes the observed preparation, we have $f(i,j) = \frac{1}{n}{}^{(0)}O(\mathbf{F}_{ij})$. This method is called the method of constant height cuts (see Fig 9b).

Furthermore, I generalised the notion of linear filters known from image processing. These filters can be used for the construction of the above-mentioned function. A function filtered in this way approximate an observed preparation essentially better. This construction method is called the method of filtered cuts. In Figure 9a, we can see a spatial reconstruction that uses a low-pass filter.

9. Spatial Reconstruction by the Method of Direct Height Determination

In the above, we used the focussing criteria as a quality characteristic. We determined the pixel altitude according to the maximum of the focussing criterion. In this way we can only obtain n levels from n focal images. However, the radius of the Euclidean trace and wave trace of the point depend on the distance of this point from the sharpness plane. The radius of these traces increases with the distance from the sharpness plane but this dependence is nonlinear. The focussing criteria parameters are changed according to this. Analysing the focussing criteria parameters for all the particular images we can determine this distance for each pixel more exactly than in the previous chapter. In this way, it is possible to obtain a 3-D object profile very easily.

Let $\mathcal{G}$: $P_3 \to P_3'$ be a geometric projection where $P \in \omega \Rightarrow \mathcal{G}(P) = P' \in \varphi_2$; $Q \notin \omega \Rightarrow \mathcal{G}(Q) = Q' \notin \varphi_2$. For the Euclidean traces $\mathcal{S}_E^P$; $\mathcal{S}_E^Q$ of the points $P \in \omega$; $Q \notin \omega$, we have the following implication: if $\mathcal{S}_E^P = \{P'\}$, then $d(\mathcal{S}_E^P) = 0$; $d(\mathcal{S}_E^Q) > 0$. Let ${}^{(k)}X{:}F_y \to \mathbf{R}$; $k = 1,..,n$ be a focussing of the image ${}^{(k)}O$ from the multifocal image O, $v({}^{(k)}X)$, $D({}^{(k)}X)$, $T({}^{(k)}X)$ the values of the variation, dispersal and frequency criteria on the same image ${}^{(k)}O$, respectively. We introduce the following denotations:

$$v\left({}^{\max}X\right) = \max\left\{v\left({}^{(k)}X\right);{}^{(k)}O \in O\right\};$$
$$D\left({}^{\max}X\right) = \max\left\{D\left({}^{(k)}X\right);{}^{(k)}O \in O\right\};$$
$$T\left({}^{\max}X\right) = \max\left\{T\left({}^{(k)}X\right);{}^{(k)}O \in O\right\}.$$

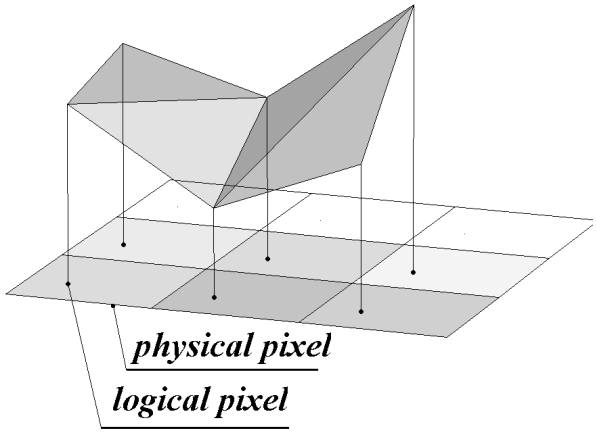

FIG. 8 Mapping of the physical plane.

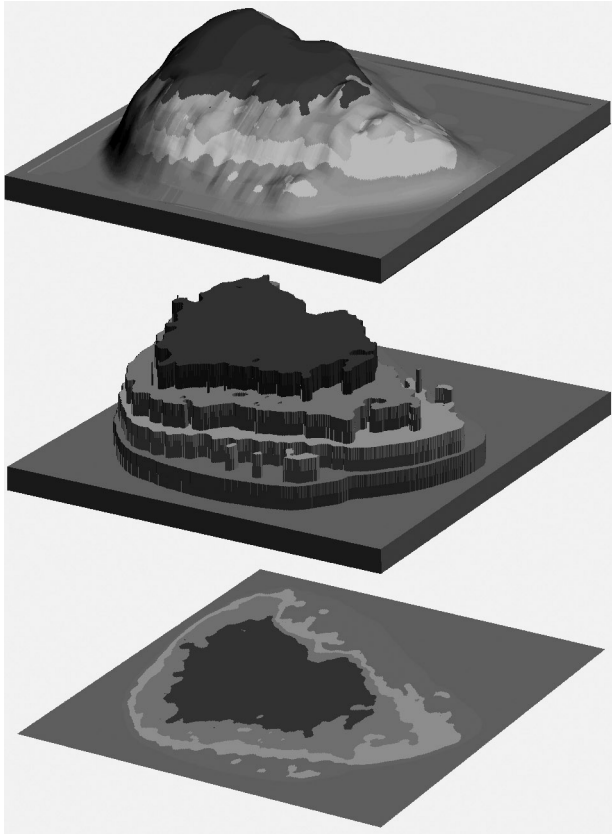

FIG. 9 Method of constant height cuts and fitered cuts.

When using the method of direct height determination, we assume that the values of the focussing criteria depend on the average the Euclidean trace $d({}^{(k)}\mathcal{S}_E^Q)$ of the point Q in the Euclidean scanning ${}^{(k)}\mathcal{M}_E$ or on the length ${}^{(k)}\ell$ represents this average. This means that there exist functions $v({}^{(k)}X) = f_v({}^{(k)}\ell)$, $D({}^{(k)}X) = f_D({}^{(k)}\ell)$, $T({}^{(k)}X) = f_T({}^{(k)}\ell)$ and their inverses $f_v^{-1}, f_D^{-1}, f_T^{-1}$. These inverse functions determine the diameter of the Euclidean trace using the focusing criteria values:

$$
\begin{aligned}
{}^{(k)}\ell = f_v^{-1} = c \cdot \frac{v\left({}^{\max}X\right)}{v\left({}^{(k)}X\right)} \; {}^{(k)}\ell = f_D^{-1} \\
= c \cdot \frac{D\left({}^{\max}X\right)}{D\left({}^{(k)}X\right)} \; {}^{(k)}\ell = f_T^{-1} = c \cdot \frac{T\left({}^{\max}X\right)}{T\left({}^{(k)}X\right)}
\end{aligned}
\tag{4}
$$

Next we have derived the dependence of the diameter d of the Euclidean trace $\mathcal{S}_E^Q$ of the point $Q \notin \omega$ on its distance h from the sharpness plane. From Figure 10 we obtain:

$$
\Delta P' F_2 F_1' \sim \Delta P_x H_1 F_1' \Rightarrow \frac{s}{f} = \frac{s'}{\Delta} \Rightarrow s = \frac{s'f}{\Delta} \tag{5}
$$

$$
\Delta Q_\varphi F_2 H_1 \sim \Delta H_1 P_x Q \Rightarrow \frac{\Delta + f}{s'} = \frac{\delta + f + h}{s} \tag{6}
$$

$$
\Delta P' F_2 H_1 \sim \Delta H_1 P_x P \Rightarrow \frac{\Delta + f}{s' + \ell} = \frac{\delta + f}{s} \tag{7}
$$

After some simplifications of Eq. (5) and after substituting from Eqs. (7) and (5), we obtain:

$$
\frac{\Delta + f}{s'} = \frac{\delta + f}{s} = \frac{h}{s} \overset{(7)}{\Rightarrow} \quad \frac{\Delta + f}{s'} = \frac{\Delta + f}{s' + \ell} + \frac{h}{s} \overset{(5)}{\Rightarrow}
$$

$$
\frac{\Delta + f}{s'} = \frac{\Delta + f}{s' + \ell} + \frac{h\Delta}{s'f}
$$

Calculating h from the last equation, we have

$$
h = \frac{\ell \, f(\Delta + f)}{\Delta(s' + \ell)}
$$

In the event that the main plane distance χ_1 to point Q is smaller than the distance from the sharpness plane, we proceed in an analogous manner to obtain the same result.

Using this expression together with Eq. (4), we can directly determine the distance of a given pixel from the sharpness plane, which yields a 3-D reconstruction of the preparation.

10. Results and Applications

We have written a program based on the above theory. It can process partially focussed images (optical cuts) and makes 2-D reconstructions (focussing) as well as 3-D reconstructions (spatial modelling). The input data can produced by any device with a very small sharpness zone (conventional microscope, CCD camera, etc). This program does not require much in the way of hardware. As a minimum, an IBM-compatible PC (IBM, White Plains, M.d., USA), with a 433 MHz processor and 64 MB RAM is recommended. It runs on lower-level PC models as well, but the run time may be too long. The run time depends on the number of the optical cuts processed, their resolution, the criterion chosen, and the processing parameters. For instance, if we process four optical cuts with a resolution of (500,435), we use a variation criterion with $\varepsilon = 4$ and the method of direct height determination, the run time of different computers is shown in Table I:

The following figures depict 3-D output data from this program. Figure 11 shows a reconstruction of an *Astrophytum Ornatum* cactus seed with four optical cuts (the processing time of this operation can be seen in Table I. A Meopta Meogon 5.6/60 mm lens was used to take the images (Meopta, Prerov, Czech Republic).

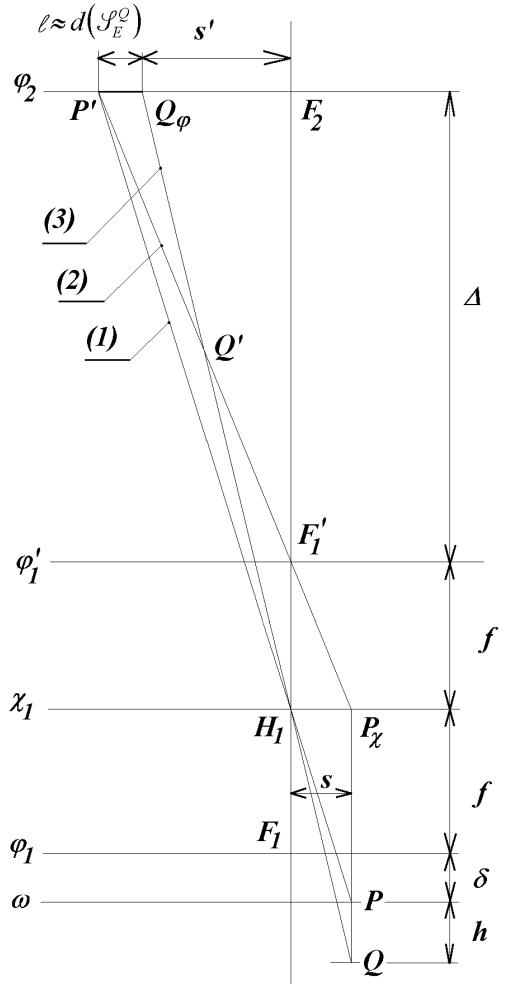

FIG. 10 Principle of spatial reconstruction by method of direct height diagnosis.

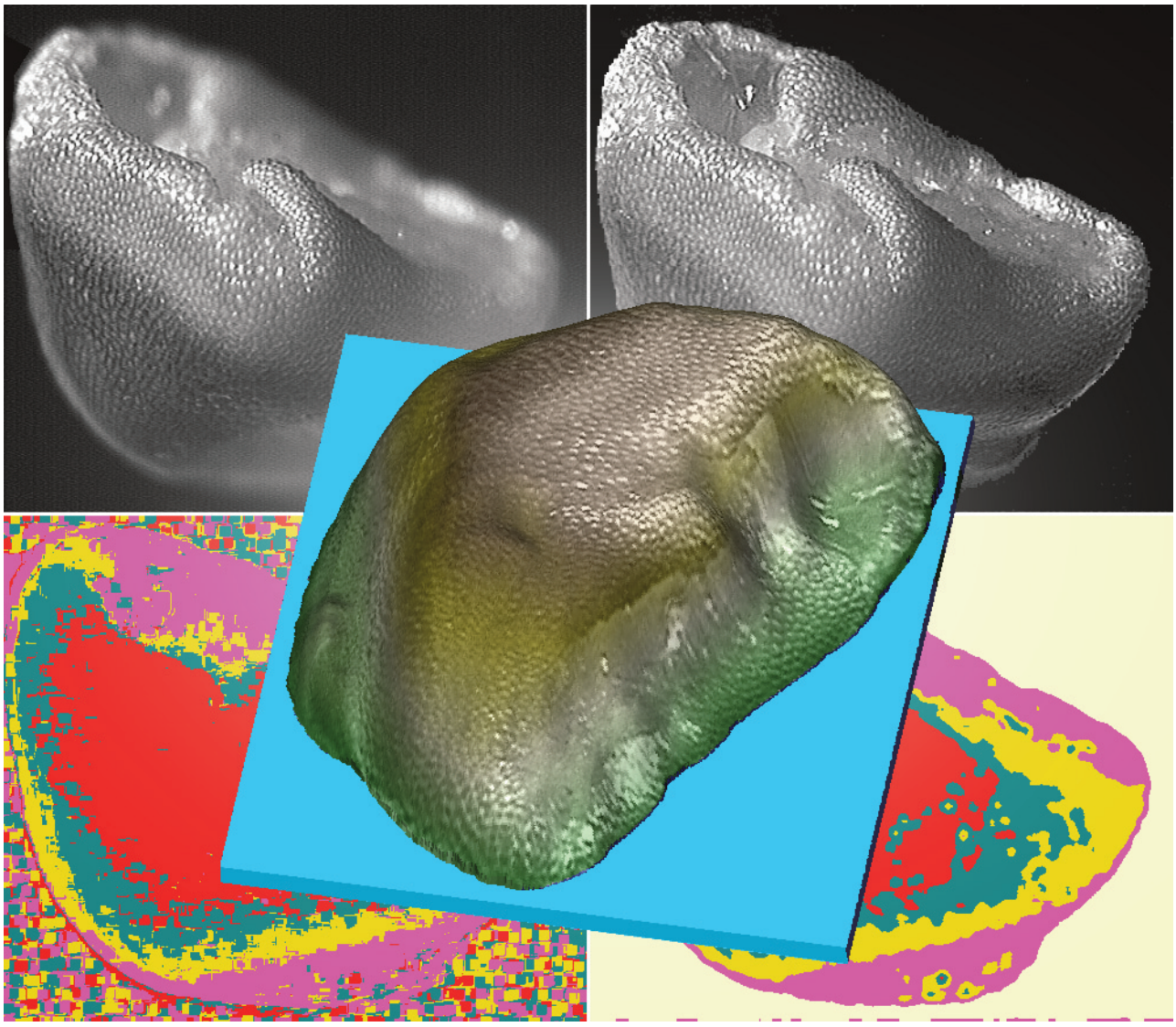

FIG. 11 Three-dimensional reconstruction of *Astrophytum Ornatum* cactus seed by method of direct height determination.

In Figure 12, we can see some of the input data on a lava fragment (data—CCD Camera Olympus DP 10, in complete eight images (Olympus America, Inc., Melville, N.Y., USA) and its 3-D reconstruction. In Figure 13a, a 3-D reconstruction is seen that uses the method of direct height determination at viewing angles of 30° and 40°. Reference microphotograph of this fragment is shown in Figure 13b at the same angles (the original fragment size is about 5 mm).

In Figure 14 we can see the input data of *Drosophila* fly (in complete eight images) (a) and a 2-D reconstruction (b). The frequency criterion was used in this construction. Figure 15 shows the 3-D output produced by our program. Figures 16 and 17 show the input data of a copper sulphate crystal (in complete 10 images) and the results of their 2-D and 3-D processing (the result is obtained by the dispersion criterion).

TABLE I The reconstruction run time at different computers

IBM PC compatible	2-D reconstruction	3-D reconstruction	full time
proc. 100 MHz, 32 MB RAM	12 min	29 min	41 min
proc. 433 MHz 64 MB RAM	1 min 15 sec	3 min 10 sec	4 min 25 sec
proc. 999 MHz 128 MB RAM	19 sec	74 sec	93 sec

Program requires about 150MB disk space per runtime. A demo-version is available at http://www.martisek.webzdarma.cz.

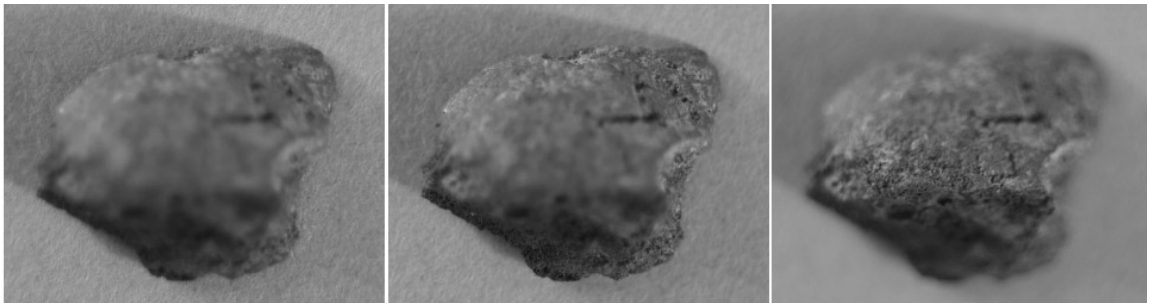

FIG. 12 Input data for three-dimensional reconstruction of the lava fragment

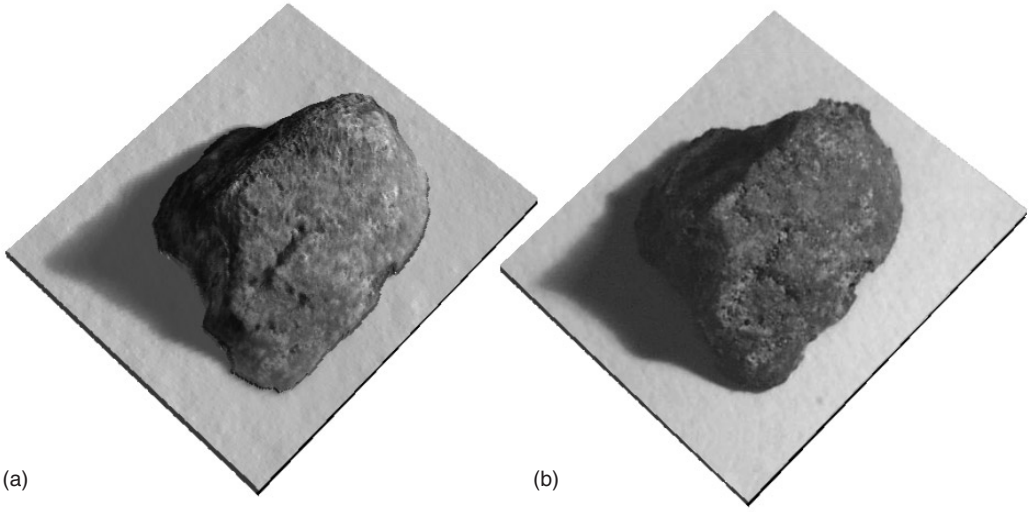

FIG. 13 3-D reconstruction and 3-D photo of the lava fragment

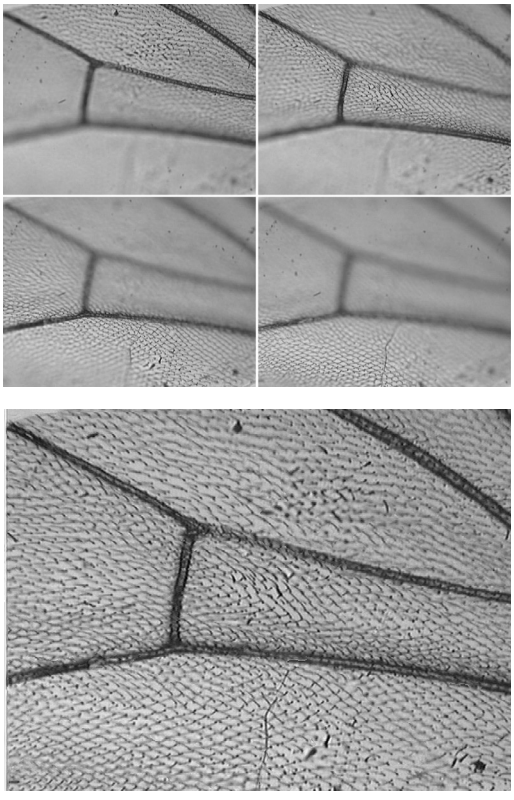

FIG. 14 Input data and sharp image of *Drosophila* fly.

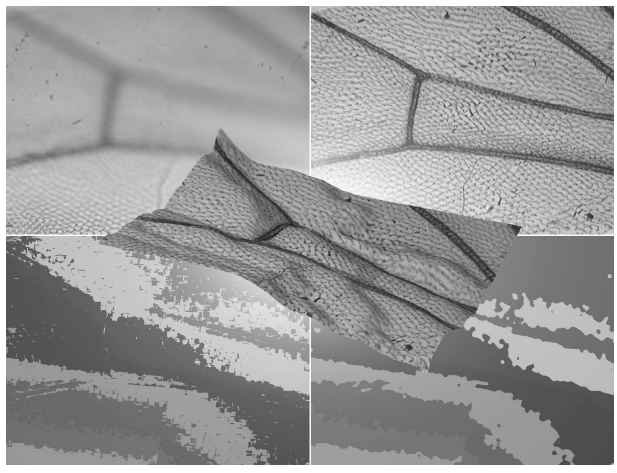

FIG. 15 Three-dimensional output of *Drosophila* fly.

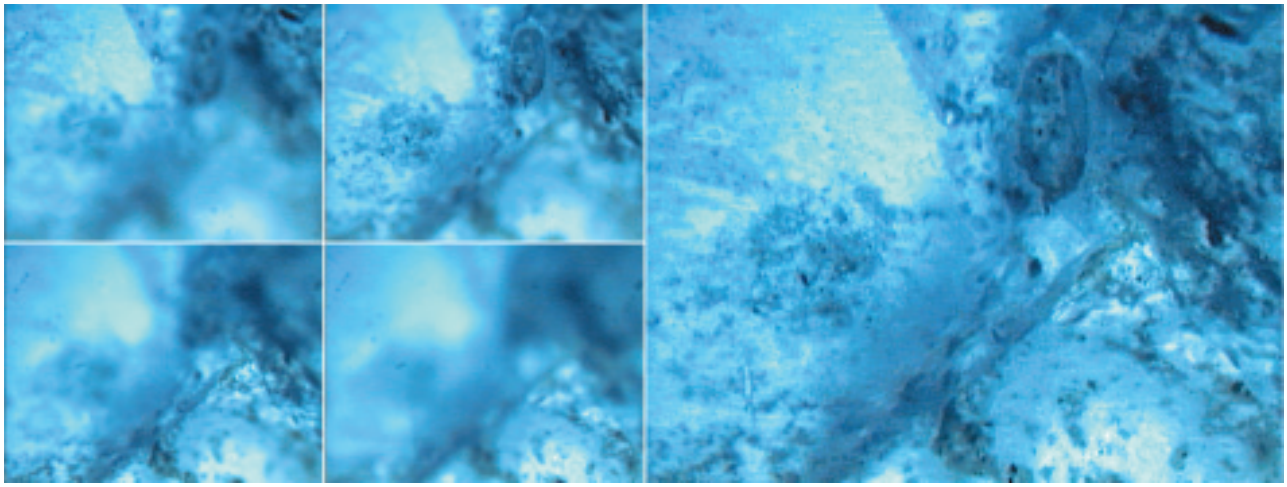

FIG. 16 Input data and sharp image of a copper sulphate crystal.

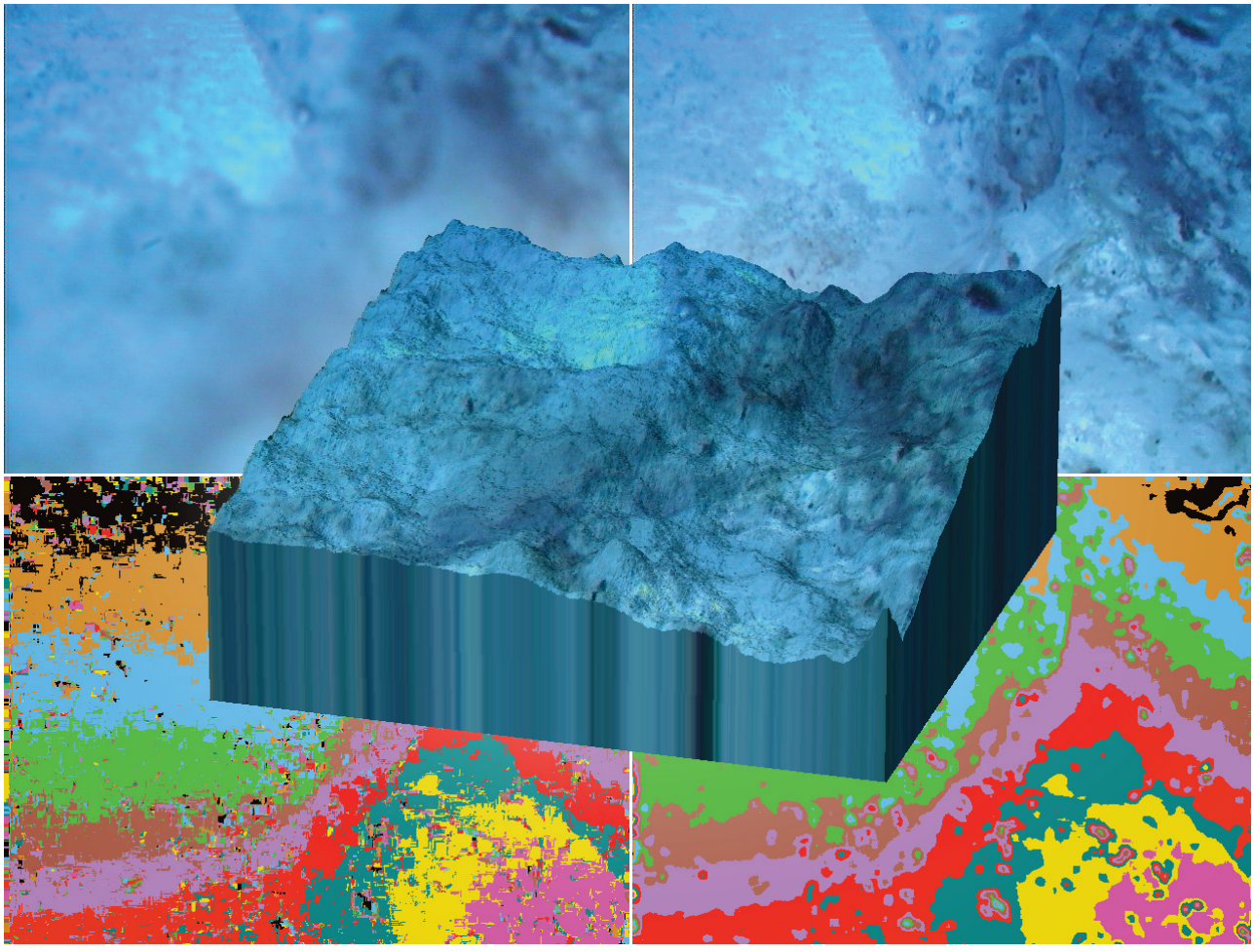

FIG. 17 Three-dimensional output of the copper sulphate crystal.

Acknowledgements

The input data produced by Mr Miloslav Druckmüller and Mr Pavel Štarha were used in this paper. The author thanks them very much for their cooperation.

References

Benson KB: *Television Engineering Handbook,* 2nd Ed. New York (1986)

Druckmüller M, Štarha P: ACC 4.0 Scientific object structure and object analyser, *SOFO Brno*, 1–103 (2000)

Druckmüller M, Heriban P: Scientific Image Analyser DIPS 5.0. *SOFO Brno,* 1–266 (1996)

Foley JD, van Dam A, Feiner SK, Hughes JF: *Computer Graphics: Principles and Practice*, 2nd Ed. Addison-Wesley, Reading, MA (1990)

Galbraith W: Letters to the Editors, Rebuttal on novel method for stereo imaging in light microscopy at high magnifications by Greenberg G. and Boyde A. *Neuroimage* 2, 85–87 (1995)

Geldziler B, Hewitt CW, Doolin EJ, Pro E: Depth of field of mycology specimens using high definition 3-D microscopy employing multiple oblique illumination. (abstr.) *Amer Soc Microbiol,* 270 (1998)

Geldziler B, Ramsamooj R, Catalano E, Doolin EJ, Hewitt CW: Novel high definition 3-D microscopy for evaluating cytopathology and pap smear specimens: 3-D digital image reconstruction and analysis of cell clusters. (abstr.) *Acta Cytologica*, 42(5), 1299 (1998)

Geldziler B, Ramsamooj R, Greenberg G, Doolin EJ, Hewitt CW: Use of 3-D microscopy with multiple oblique illumination in evaluating cytopathology preparations. (abstr.) *Analytical Quantitative Cytol Histol* 193 (1998)

Greenberg G: Direct 3-D imaging using a multiple oblique microscope. *Scanning* 16, 248–249 (1994)

Greenberg G, Boyde A: Convenient and controllable direct-view 3-D imaging in conventional light microscopes: Approaches via illumination and inspection. *Proc RMS* 32/2, 87–101 (1997)

Greenberg G and Boyde A: Direct-view 3-D microscopy using conventional lenses. *Microsco Anal* 22:7–9 (1997)

Hewitt CW: Evaluation of various conventionally and immunostained specimens by novel high definition 3-D microscopy. (abstr.) *Proc Joint Meeting Histochem Soc and Japan Soci Histochem and Cytochem* A6 (1998)

Hewitt CW, Goodman M, Tarnoff M, Doolin EJ: Mathematical evaluation of high definition 3-D microscopy using digital imaging. (abstr.) FASEB Journal, Vol. 11(3), A636 (1997)

Hewitt CW, Geldziler B, Ramsamooj R, Greenberg G, Doolin EJ: *High definition Microscopy Based on Multiple Oblique Illumination for Cytopathology and Pap Smear Analysis: Evaluation of 3-D Digital Image Reconstruction and Analysis.* A communication: 11th International Congress on Diagnostic Quantitative Pathology. Sierra ñ Italy (1997)

Hewitt CW, Salartash K, Dalsey RM, DeLong WG: Cellular changes in the joints of composite tissue allograft recipients analyzed by computerized digital image processing and a 3-D microscope. (abstr.) *FASEB J*, 9(3), A434 (1995)

Netravali AN, Haskel BG: *Digital Pictures Representation and Compression*. Plenum Press, New York, NY (1988)

Roger DF, Adams JA: *Mathematical Elements for Computer Graphics*, New York (1985)

Seyedolali A, Torley RF, Krinsley D, Boggs S Jr: Three-dimensional, high-resolution light microscopy—a new geological tool. *J Geolog Ed* 42, 5, 476–480 (1994)

Watt A: *Fundamentals of Three-Dimensional Computer Graphics*, Addison Wesley, Reading, MA (1989)